Chapter 5

Through-Vial Impedance Spectroscopy (TVIS): A New Method for Determining the Ice Nucleation Temperature and the Solidification End Point

Geoff Smith[a] and Yowwares Jeeraruangrattana[b]

[a] Leicester School of Pharmacy, De Montfort University, Leicester, LE1 9BH, United Kingdom

[b] Research and Development Institute, The Government Pharmaceutical Organization (GPO), Thailand

Author	Geoff Smith and Yowwares Jeeraruangrattana
Chapter title	Chapter 5 Through-Vial Impedance Spectroscopy (TVIS): A New Method for Determining the Ice Nucleation Temperature and the Solidification End Point
Book	Freeze Drying of Pharmaceutical Products
Editors	Davide Fissore, Roberto Pisano, and Antonello Barresi
Publication date	November 12, 2019
Publisher	CRC Press LLC
ISBN	978036707680

Cite as:

Smith, G. & Jeeraruangrattana, Y. 2019, "Chapter 5 Through-Vial Impedance Spectroscopy (TVIS): A New Method for Determining the Ice Nucleation Temperature and the Solidification End Point" in Freeze Drying of Pharmaceutical Products, eds. D. Fissore, R. Pisano & A. Barresi, 1st edn, CRC Press, Florida, United States, pp. 77-98.

An Introduction to Through Vial Impedance Spectroscopy

Through vial impedance spectroscopy (TVIS) as the names suggests measures the electrical impedance spectrum of a solution through the walls of the container in which the solution is freeze-dried. The location of the electrodes on the outside of the container means that the technology is non-product invasive and therefore the impact on nucleation, ice growth, heat transfer and dry rates is minimized. With the current design of the TVIS impedance analyzer, a single pair or multiple pairs of electrodes are physically attached to the outer wall of the container (a glass vial or ampoule) (***Figure 1a***). The low thermal mass and streamlining of the external electrodes, which are connected to fine 'flexible' coaxial cables (not shown) means that the technology is also non-perturbing to the packing of the vials in the dryer (thereby maintaining the inherent heat transfer characteristics to the vials).

From an electrical impedance perspective, the TVIS vial can be regarded as a composite object, comprising two arc sections from the glass wall of a vial, in series, with a cylinder of ice (***Figure 1b***). The impedance of each component is represented by a complex capacitances ($C^* = C' - iC''$). The complex capacitance of the glass wall is characterized by (1) a frequency dependent component (a low frequency dispersion) which can be modelled over a limited range of frequencies by a constant phase element, and (2) a frequency independent component modelled by a simple capacitor. The complex capacitance of the ice cylinder is characterized by (1) a dielectric relaxation that can be modelled by a Cole-Cole dispersion and (2) a frequency independent component modelled by a simple capacitor. For both components, the frequency independent capacitances model the instantaneous electronic and atomic polarizations of the glass wall and the ice, respectively.

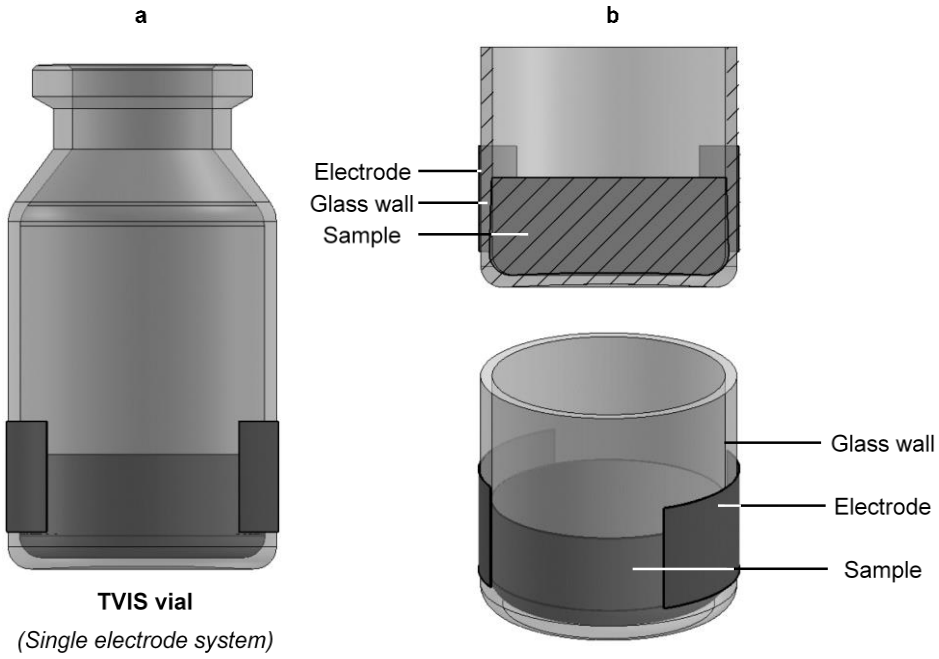

Figure 1 (a) Sketch of a TVIS vial with a pair of 19 x 10 mm electrodes attached to the external wall of the vial and positioned of 3 mm from the base. (b) 3D sketch of the segment of glass and sample which is measured in the TVIS impedance spectrum.

Impedance spectra are generated throughout the drying cycle and displayed in terms of the two components of the equivalent complex capacitance spectra, i.e. the real capacitance (dielectric storage) (***Figure 2a***) and imaginary capacitance (dielectric loss) (***Figure 2b***). The example spectrum given here is for a TVIS vial containing ice at −20 °C. The complex capacitance spectrum has a frequency response which is due to the low frequency dispersion of the glass wall impedance at low frequencies (< 100 Hz or log frequency = 2, ***region I in Figure 2***). Then as the impedance of the low frequency dispersion decreases, as the frequency of the excitation signal increases, it gives way to a pronounced dielectric relaxation of ice that dominates the majority of frequency range of the TVIS complex capacitance spectrum. For the current design of analyser, this experimental frequency window extends from 10 Hz to 1 MHz. The dielectric relaxation of ice (whether measured through the glass vial or in the more conventional approach of using planar metal electrodes) spans three log decades in frequency (100 Hz to 100 kHz, ***region II in Figure 2***) and is manifest as a step-change in the real part spectrum and a peak in the imaginary part spectrum. However, it is important to realise that, while the frequency dependence of the glass wall impedance dominates the visible characteristics of low frequency part of the spectrum, the entire

spectrum is also impacted by the series impedance of the glass wall and its interface with the contents of the vial. It follows that the real part capacitance, in the limit of either low or high frequency relative to the relaxation frequency of ice, is a function of both the glass-wall/interfacial impedance and either the static capacitance of ice (in the case of the low frequency end of the spectrum) or the instantaneous capacitance of ice (in the case of the high frequency end of the spectrum).

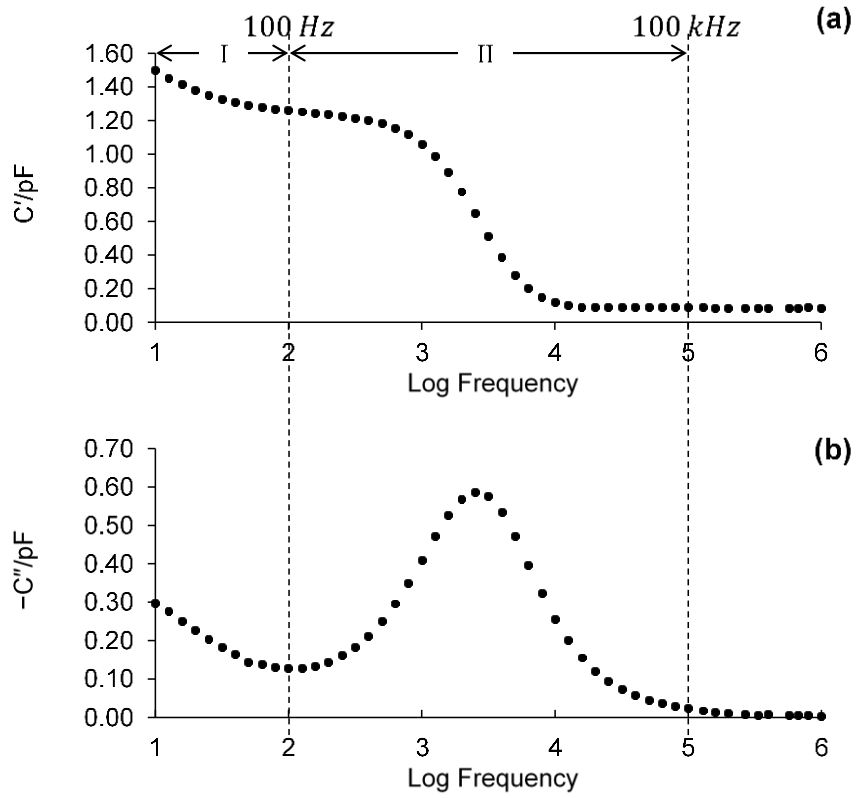

Figure 2 Real (a) and imaginary (b) components of the complex capacitance spectrum of a type I tubular glass vial with a pair of 10 x 19 mm electrodes attached to the external surface of vial and containing 3.5 g of double distilled water which has been frozen and then re-heated to – 20 °C.

One final point to make, is that although the relaxation peak observed for frozen water is due to the dielectric relaxation of ice, additional process may also occur for frozen solutions. There are two potential mechanisms that underpin the physical origin of these additional processes: the first is the dynamic glass transition (the so called α-relaxation). The second is the Maxwell-Wagner (MW) or interfacial polarization, either at the glass-wall/solution interface or the interstitial spaces between the ice crystals. These additional processes may appear separated from and usually at lower frequencies than the main relaxation of ice, or merged with the ice relaxation to form one

larger peak, whereby this larger peak presents as either a peak with a low frequency shoulder (in the case of a partially merged peak) or as a single Debye-like peak (in the case of a fully merged peak). The proximity of these additional processes to the ice relaxation peak depend on the composition of the unfrozen fraction and the temperature of the frozen solution. In one published example, our observations appear to suggest that the temperature dependence of a fully merged process (e.g. that for a 10% w/v maltodextrin solution) tends to be associated with that of the unfrozen fraction rather than the ice fraction and so may be used to determine the glass transition temperature (Smith et al. 2013, 1130-1140).

With water, and also with some solutions, it is often sufficient to follow the characteristic frequency and amplitude of the dielectric loss peaks in order to determine:

1. The suppression of eutectics by glass forming solutes (Arshad et al. 2014, 598-605),
2. The changes in ice structures that occur on annealing from which the annealing hold time may be optimized (Smith et al. 2014, 1799-1810),
3. The measurement of the average temperature of ice at a loci within the frozen volume (Smith et al. 2017, 26-40),
4. The drying rate of ice and the temperatures of ice at the sublimation interface and at the interface with the base of the vial; from which the heat transfer coefficient may be derived (Smith, Jeeraruangrattana, and Ermolina 2018, 224-235).

In other cases (to be reported in future publications) it is necessary to use a dielectric relaxation model to fit the spectra and to separate out the contributions from the ice and the unfrozen factions. These features of impedance spectroscopy set it apart from other applications of impedance analysis whereby a single frequency (often using 1 kHz) is used investigate the phase changes of the solution to be freeze-dried, (in an approach which is akin to that used in thermal analysis whereby the pre-frozen solution is re-heated in order to observe its phase behaviour.

TVIS Applications – An Overview

The idea that it might be possible to measure the freeze-dried contents of a glass vial, with electrodes positioned on the outside of the vial, was first evaluated by Suherman et al (Suherman 2001; Suherman, Taylor, and Smith 2002, 337-344). The materials under test were primarily hydrated proteins, e.g. ovalbumin and lysozyme and the 2-3 dielectric relaxations observed were considered to be due to either the Maxwell-Wagner polarization of the glass wall or the relaxations of localized proton percolation through the hydration shell of the protein. The work was influenced by Careri et al (1985) who studied freeze-dried lysozyme in a glass dish with parallel plate electrodes. Later, and stimulated by a collaboration between De Montfort University and GEA Pharma Systems, work started on the evaluation of the use of external electrodes to monitor the freeze-drying process (Innovate UK Collaborative R&D project grant, LyoDEA 100527). That project led to a bespoke impedance analyzer that was specifically designed for the purpose of measuring the dielectric properties of solutions undergoing a freeze-drying process from a glass vial (Smith and Polygalov 2019).

Applications for TVIS in the development of a freeze-drying process can be divided into qualitative studies and quantitative studies.

Qualitative studies largely involve the study of the onset or end point of some stage of the process, e.g. (1) the ice nucleation event, (2) the completion of ice formation and/or the formation of eutectics during the solidification/freezing phase; (3) the completion of any recrystallization (Ostwald ripening) during an annealing stage; (4) the observation of collapse; and (5) the end point of primary drying.

Quantitative studies (which require some form of calibration) include: (1) the prediction of ice temperatures during primary drying and (2) the determination of the glass transition temperatures, (3) the determination of the sublimation rate in primary drying; from which critical process parameters may be derived, including the vial heat transfer coefficient and the product dry layer resistance. Other applications might be conceived for the secondary drying stage but these will be the subject of future studies.

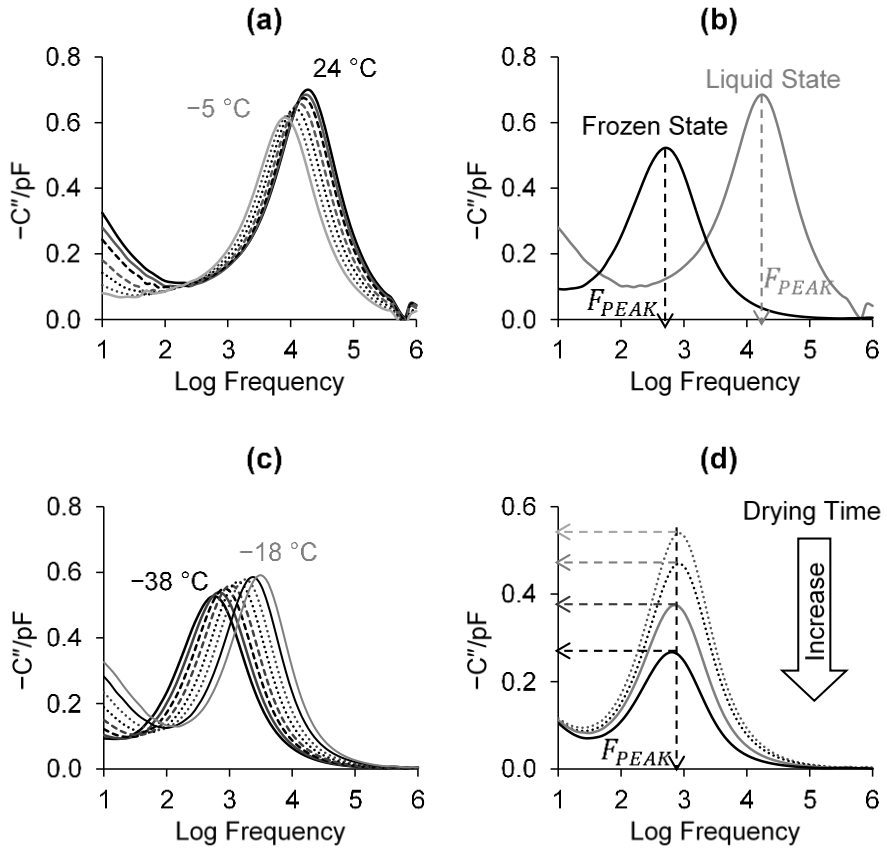

Figure 3 Basic responses of TVIS dielectric loss spectrum of double distillation water 3.5 g containing in a type I tubular glass vial with a pair of 10 x 19 mm electrodes attached to the external surface of vial during freeze drying process: (a) cooling the liquid phase, (b) phase transition (liquid water to ice), (c) heating of the solid phase, and (d) primary drying.

Figure 3 summarizes the basic responses of the TVIS dielectric loss spectrum of a water-filled vial to the processes of (a) cooling the liquid phase, (b) phase transition (liquid water to ice), (c) heating of the solid phase, and (d) primary drying. Any changes in the dielectric loss peak due to the relaxation of ice are mirrored in the step in the dielectric storage (as was demonstrated in ***Figure* 2)** but given that it is easier to see the relative changes in the frequency and dielectric strength of a relaxation process in the form of a peak then these first explorations of the potential applications for TVIS in ***Figure 3*** show only the dielectric loss peak.

In the liquid state the dielectric loss peak appears at first glance to be similar to the dielectric relaxation of ice. However, this relaxation is due to an entirely different relaxation process known as a Maxwell-Wagner polarization or interfacial polarization, which occurs at the extremes of the physical geometry of the sample. In other words, there is an accumulation of charge (polarization) at the interface between the glass wall and the water (where the charges originate

from mobile ionic species in the water). As stated earlier, the impedance of the glass wall is impacted by the interfacial layer that forms between the glass and the solvent, and so it follows that a study of this interfacial impedance provides one possible assessment of the nature of the interaction between different liquid and the glass.

The temperature dependence of the characteristic relaxation frequency (F_{PEAK}) of the Maxwell-Wagner relaxation (***Figure 3a***) is largely due to the temperature dependence of the electrical resistance of the water. However, when frozen the shift in the characteristic frequency towards lower frequencies (***Figure 3b***) is due to the formation of ice (which itself has a dielectric relaxation) rather than the increase in resistance associated with the formation of the solid phase. The electrical resistance of the sample is now much higher than in the liquid state so we expect that the Maxwell-Wagner polarization of the interface between the glass wall and the ice will be shifted to frequencies below the lower limit of the experimental frequency window.

The dielectric relaxation time of ice increases as the temperature is reduced and so the peak shifts to lower frequencies. The peak frequency (F_{PEAK}) therefore provides a surrogate measurement for the ice temperature (***Figure 3c***). The calibration of this TVIS parameter for temperature may be achieved by introducing a temperature cycling stage (of reheating and re-cooling) once the ice has been frozen from the solution.

The height of the relaxation peak (C''_{PEAK}) is proportional to the height of the ice cylinder in direct contact with the inside of the glass wall. For a cylindrical ice mass (where the volume and therefore mass is proportional to the ice cylinder height) it follows that he TVIS parameter C''_{PEAK} may be calibrated for ice mass thereby provide an opportunity to measure the drying rate in primary drying (***Figure 3d***). The caveat, however, is that in both cases of temperature and ice mass predictions during primary drying (using electrodes attached to the wall of the vial) the ice cylinder (which is defined in part by the shape of the sublimation interface) must not change shape as the ice cylinder reduces during the sublimation process. This condition is met for the freeze-drying of ice formed from solutions, and especially for those core vials at the center of the shelf, but only holds true for a limited period of time for the freeze-drying of ice which is formed from pure water. This requirement is likely to be less important in future applications of TVIS where the electrodes

are removed from the vial and replaced by a single electrode placed above the vial(s), which then measures through the vial base to the freeze-dryer shelf (the ground plane).

In this chapter we devote our attention to the application of TVIS to:

1. The calibration of the liquid state and solid state temperatures,
2. The identification of the two critical events in the freezing stage of the lyophilization cycle, i.e. the determination of the ice nucleation temperature and the end of solidification phase.

It should be recognized that the ice nucleation temperature and the solidification end point may in fact be determined in one relatively straightforward manner, by using a thermocouple placed within the vial. And so that begs the question as to whether there is a need for an alternative technology for this purpose. The reason for an alternative technology is that the very presence of the thermocouple alters the way in which the ice freezes and therefore changes the ice crystal structures (Roy and Pikal 1989, 60-66). It follows that the thermocouple containing vial is non-representative of those vials in its locality during the freezing stage. This is equally true for the primary drying stage whereby the drying rate is affected by the altered ice structures (which impact the vapour flow resistance of the dry layer) and the additional heat source provided by the thermocouple.

Temperature Calibration of the TVIS system

First, we shall concentrate on methods for calibrating the TVIS response for the temperature of the liquid state (prior to the onset of ice formation, i.e. ice nucleation).

The obvious way to approach the calibration of the TVIS response for temperature would be to place a temperature sensor such as a thermocouple inside the vial (notwithstanding what has just been said about the impact of the sensor on ice crystal structures). Unfortunately, because the metal of a hardwired thermocouple[1] is electrically grounded, it introduces a significant distortion in the impedance spectrum if one attempts to measure the TVIS response while the thermocouple remains inside the vial and in contact with the liquid (***Figure 4***). We note here that this perturbation is much less for ice or a frozen solution.

There are a number of approaches that might address this issue:

1. The use of temperature sensors in nearest neighbor vials to infer the product temperature in the test vial.
2. The use of non-metallic sensors (based on fiber optic technology) or wireless sensors (such as Tempris®).
3. The use of planar thermocouples attached to the outside of the vial (Parvis, Grassini, and Barresi 2012, 1994-1998; Grassini, Parvis, and Barresi 2013, 1276-1283; Parvis et al. 2014, 1465-1470).

[1] As opposed to those temperature sensors that are operated wirelessly

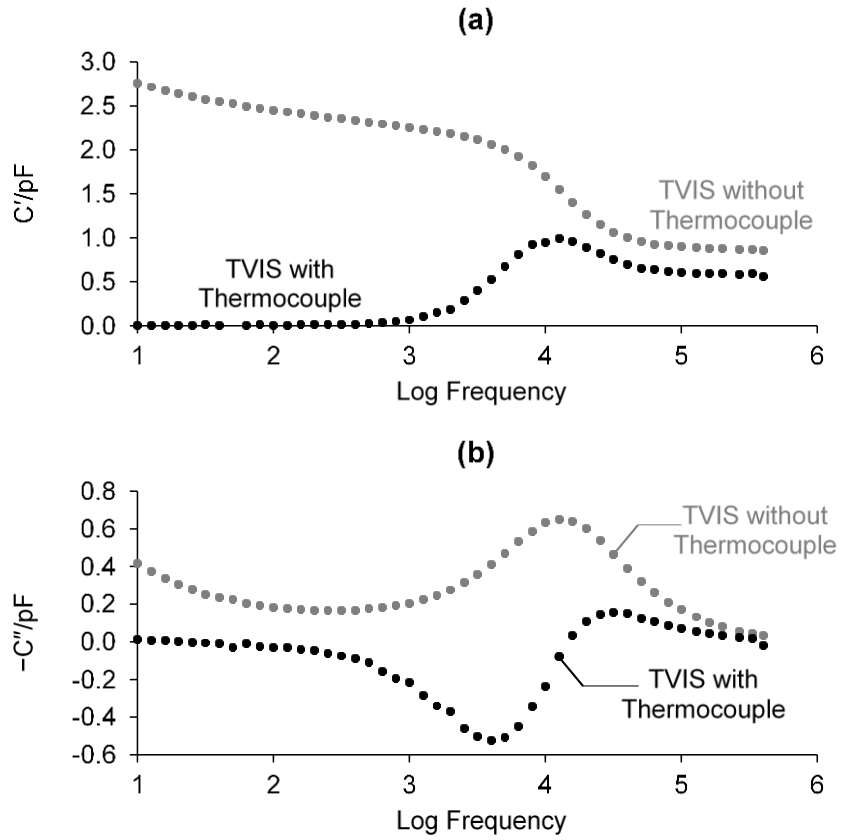

Figure 4 (a) Real part spectra and (b) imaginary part spectra showing the impact on the TVIS spectrum of a thermocouple placed within a TVIS vial of containing ultrapure water relative to without one.

Here we describe the first two of these approaches:

The first approach is to use temperature measurements in the nearest neighbor vials (i.e. those vial in close proximity of the TVIS vial and at a height which corresponds to the center point of the ice layer in the region bounded by the electrode) in order to predict the product temperature in the TVIS vial (***Figure 5***). The thermocouples used should comply with best practice for wired sensors as defined by Nail et al. (2017). The disadvantage of the approach is that there is invariaby a distribution in temperatures between vials and therefore this approach will inevitably introduce some uncertainty in the calibration of F_{PEAK}. This uncertainty can be determined by taking half of the range of temperatures recorded in a minumum of three of the nearest neighbour vials. Typically this range is in the region of 0.4 °C so an uncertainty limit might be in the region of +/− 0.2 °C. The advantage, however, is that it avoids having an invasive temperature sensor in the vial which provides another heat source and additional nucleation sites that.would otherwise impact the way the ice freezes and dries.

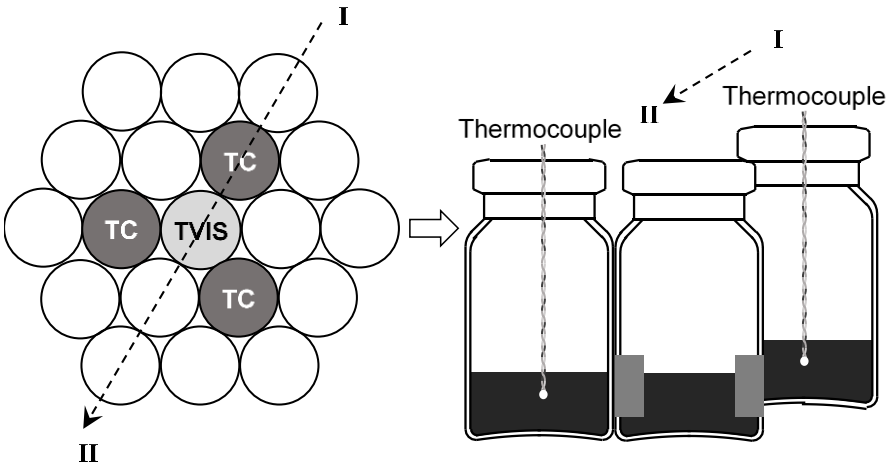

Figure 5 Triangulation method for temperature calibration of the TVIS vial showing a schematic of the position of three thermocouple containing vials (marked TC) as nearest neighbors for the TVIS vial (marked TVIS). The triangulation of temperature measurements may be used to infer the temperature of the material inside the TVIS vial to an accuracy which is approximately equal to the deviation from the mean thermocouple temperature at any point in time during the reheating of the population of vials.

The second approach is to place a non-metallic element, such as a fibre optic probe with a Bragg grating or a wireless temperature sensor based on a quartz crystal resonator (Tempris®) directly in the TVIS test vial. Fibre optic sensors have been used previously in freeze-drying applications (Friess, Resch, and Wiggenhorn 2010; Kasper et al. 2013, 449-459; Horn and Friess 2018) and are shown in our studies to be non-perturbing to the TVIS spectrum. Wireless sensors (Schneid and Gieseler 2008, 729-739) are becoming commonplace in freeze-drying production applications and in our studies are also shown to be non-perturbing to the TVIS spectrum (***Figure 6***).

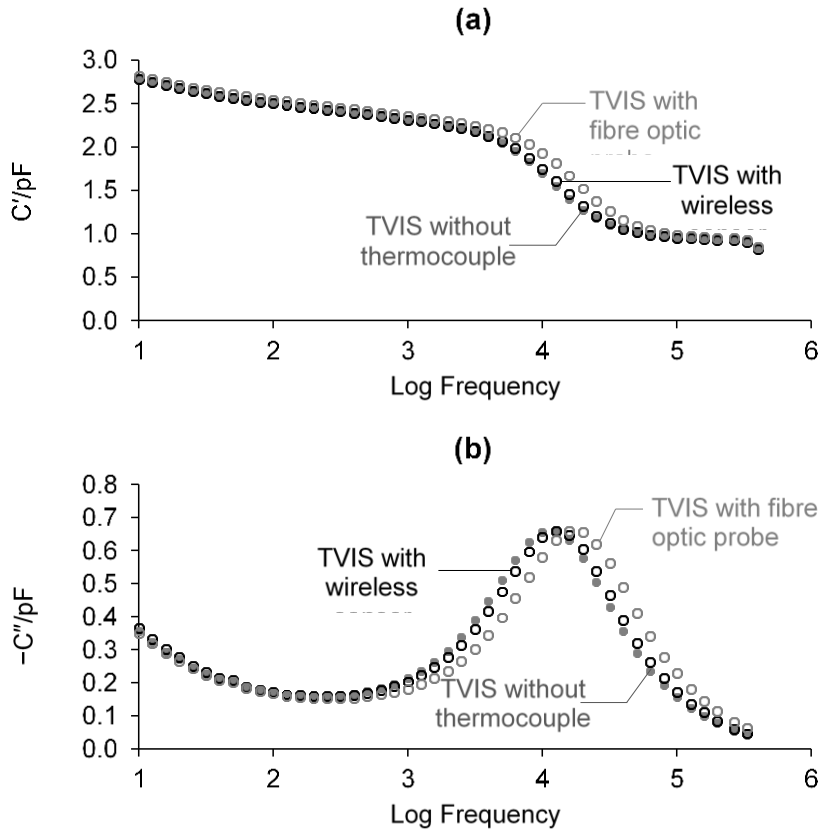

Figure 6 The similarity in shape of real part spectra (a) and imaginary part spectra (b) of ultrapure water between a TVIS vial with a fibre optic sensor, a wireless sensors (Tempris®) and the same vial without any temperature sensors.

By modeling (Smith et al. 2017, 26-40) it has been demonstrated that $\log F_{\mathrm{PEAK}}$ is dependent on the average temperature in the region bounded by the electrodes (assuming a linear temperature gradient across this region). Therefore in both cases of the triangulation method using nearest neighbour vials containing thermocouples (to interpolate the temperature in the TVIS vial) or the direct method with the fiber optic sensor or wireless sensor inside the TVIS vial, the tips of the sensors should be positioned at a height which is defined by the mid-point of the volume of liquid or frozen-solid in the region bounded by the electrodes (***Figure 7***). This height is given by $d_{\mathrm{m}} + d_{\mathrm{b}}$.

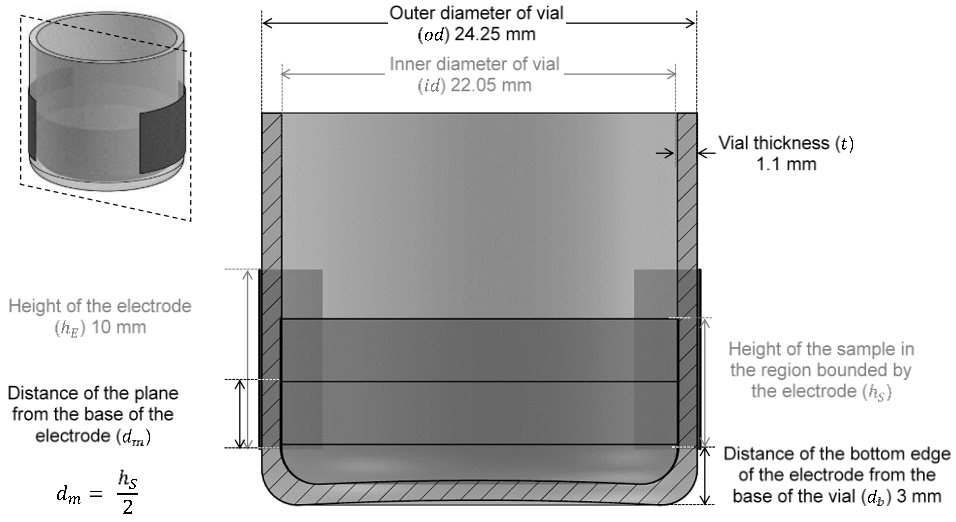

Figure 7 Illustration of a TVIS vial showing the dimensions. d_{b} : The distance of the bottom edge of the electrode from the base of the vial; h_{s} : height of the sample in the region bounded by the electrode; h_{E} : height of the electrode; d_{m} : distance of the mid-point of the sample contained within the region bounded by the electrodes from the base of the vial.

Liquid Temperature Calibration

The first application for this temperature calibration would be to exploit the temperature dependence of the Maxwell-Wagner process that is observed for the liquid filled vial. This works well for water and for solutions of neutral solutes such as the sugars, as the relaxation frequency of the MW process is well within the experimental frequency range of the current TVIS technology. Both F_{PEAK} and C''_{PEAK} have temperature dependencies of comparable magnitude and so in theory either parameter could be used. However, given that C''_{PEAK} also depends on the height of the liquid in the vial then its preferable to use F_{PEAK} for temperature calibration for water in the liquid state (***Figure* 8**).

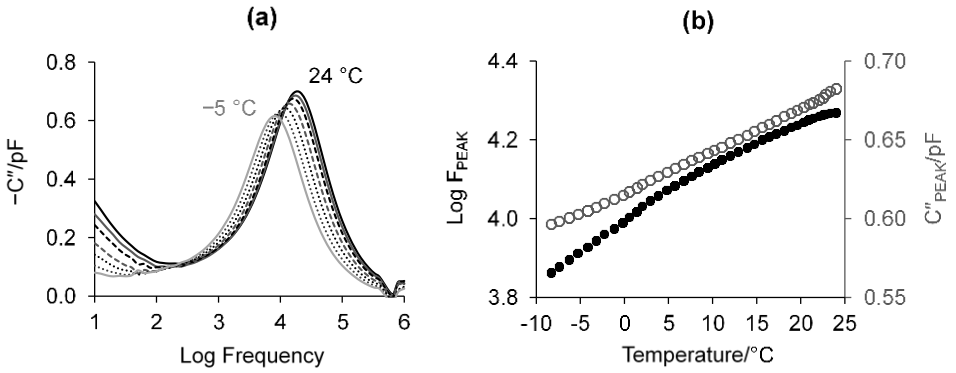

Figure 8 (a) Imaginary capacitance spectra of double distilled water inside a TVIS measurement vial (10 ml nominal capacity) with a pair of 10 x19 mm electrodes (positioned with the lower edge of the electrode at a height of 3 mm from the base of the vial. The temperatures for the selected spectra are inferred from thermocouple measurements in nearest-neighbour vials (according to the triangulation method described in the text). (b) Temperature dependencies of the TVIS parameters log F_{PEAK} (filled circle) and C''_{PEAK} (open circle) associated with the supercooling of water in the TVIS vial.

Temperature calibration for the liquid state can be incorporated within a conventional cycle, which inevitably starts with the cooling phase in order to reduce the liquid temperature to some sub-zero temperature (super-cooling) and initiate ice nucleation. For the purpose of the calibration, TVIS spectra are recorded simultaneously (e.g. every 2 min) with the recording of the temperatures from the sensors in the nearest neighbor vials as the liquid cools. It is convenient that the cooling rates employed in a conventional cycle (0.5 to 1 °C min^{-1}) are sufficiently slow that some degree of thermal equivalence in maintained between the TVIS vial and the nearest neighbor vials. Nevertheless, there will be a degree of uncertainty in the temperature predicted form the nearest-neighbour vials which is comparable with the temperature variation between those vials being used for calibration purposes. As stated earlier, this variation is typically in the region of +/− 0.2 °C and is then taken as our estimate for the uncertainty in any temperature inferred from this calibration approach, e.g. in the determination of the nucleation temperature in the freezing stage.

Ice Temperature Calibration

The sensitivity of the peak frequency (F_{PEAK}) to the temperature of the ice in the volume space bounded by the external electrodes is largely due to the temperature dependency of the dielectric relaxation time of ice. The possibility exists to calibrate this response against known product temperatures (as determined by thermocouple or RTD sensors) by the inclusion of a thermal cycling stage, after the freezing stage. Here it is the calibration coefficients for the re-heating phase of the thermal cycle (rather than the re-cooling phase) which are used to predict the temperature in primary drying ***(Figure 9)***.

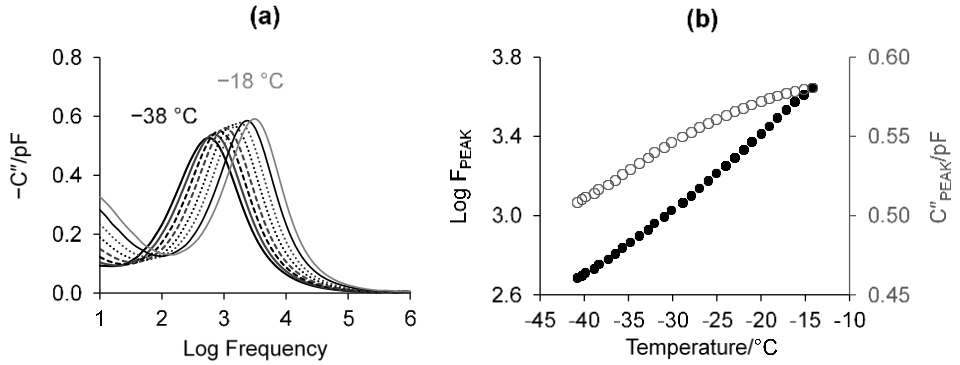

Figure 9 (a) Imaginary capacitance spectra of frozen water contained in a 10-mL type I tubular glass vial with a pair of 10 x19 mm electrodes (positioned with the lower edge of the electrode at a height of 3 mm from the base of the vial) demonstrating the temperature dependency of the dielectric loss peak of ice during the re-heating phase of a thermal cycle. The temperatures for example spectrum are interpolated from thermocouple measurements in nearest neighbor vials; (b) Temperature dependencies of the TVIS parameters log F_{PEAK} (filled circle) and C''_{PEAK} (open circle) of ice during reheating from −40 to −10 °C with 0.5 °C min^{-1} rate.

Temperature calibration is achieved having frozen the product (or water) to between −50 and −45 °C, and then holding for 1-2 h before re-heating at a slow rate (e.g. 0.5 °C min^{-1}) whilst recording both the TVIS spectra and the temperature from the sensing probes. Unlike for the liquid state, for which the calibration can be undertaken as an inherent part of the cycle, the solid state calibration however requires the incorporation of an additional thermal cycling stage.

In one case it might be that the cycle demands an annealing stage to 'ripen' the ice crystal structures and so the product temperature is taken from the solidification temperature to a temperature above T'_{g} but below the melting temperature before returning product temperature to a value below T'_{g}, prior the application of the vacuum (***Figure 10a***). Given that the impedance of

the product is likely to change as a result of annealing then it will be necessary to include an additional reheating stage which takes the product temperature back to the glass transition in order to capture the calibration coefficients for the TVIS parameter, F_{PEAK}, before almost immediately returning it to the target initial temperature prior to the application of the vacuum (***Figure 10a***). It should be noted that, before application of the vacuum the product temperature will be higher than the shelf temperature (by a few degrees centigrade) and therefore this should be taken into account when setting the shelf temperature. In other words, the shelf temperature should be a few degrees below the target product temperature (i.e. T_{g}') in order to ensure that the product doesn't anneal.

In another case it might be that the product should not be annealed in order to protect the stability of the active pharmaceutical ingredient (API) and so the product temperature is taken from the solidification temperature to a temperature below T_{g}' and then back to the target temperature prior to the application of the vacuum (***Figure 10b***). Given that a temperature cycle which maintains the product below T_{g}' is unlikely to have annealed the product (i.e. change its ice structure and hence its impedance) then it is expected that the calibration coefficients may be captured during the first reheating stage without any further recycling of the temperature.

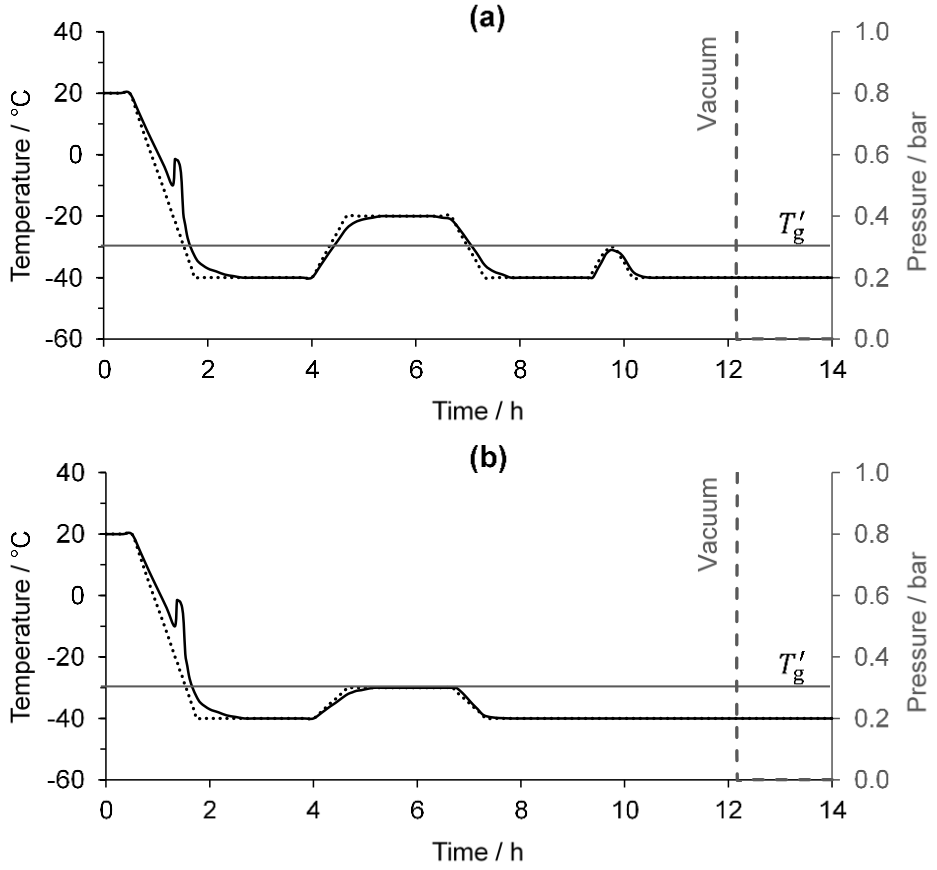

Figure 10 Examples of thermal cycles for the calibration of the TVIS system. Cycle (a) applies to the condition when the product is expected to be annealed and cycle (b) applies to the condition when the product is not supposed to be annealed. In both cases the solid black line represents the product temperature and the dotted line represents the shelf temperature

In both cases, the initial equilibrium product temperature in the initial stages of primary drying (prior to the development of the dry layer resistance) will defined by the chamber pressure and hence that lower limit of product temperature must at least be captured in the range of temperatures programmed for the thermal cycle/calibration.

Here we use a simple polynomial function to model the temperature dependency of the TVIS peak frequency associated with the dielectric relaxation of the ice. However, a more rigorous approach might be to fit the data with a Cole-Cole relaxation function in order to determine the relaxation time and then to use the equations (15 and 16) described by Popov et al. (2015, 2017) to model the characteristics (shape) of the calibration curve; a model which takes into account the cross-over behavior in the polarization mechanism of ice from orientation defect propagation at higher temperature (> 235 K) to ionic defect propagation at lower temperature (< 235 K).

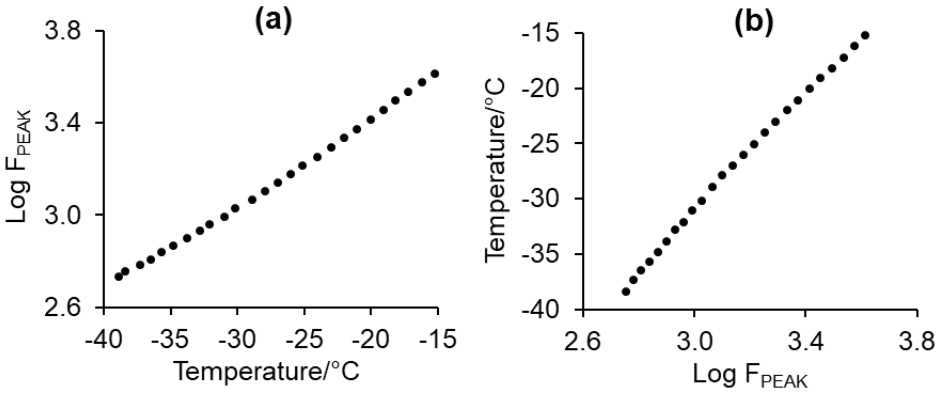

Figure 11 (a) Temperature coefficient plot of log F_{PEAK} for the ice relaxation peak vs the temperature in the nearest neighbor vial, and (b) temperature calibration plots of log F_{PEAK} for the ice relaxation peak vs the temperature in the nearest-neighbour vial. The object under test is a 10 mL glass tubing vial with a pair of 10×19 mm electrodes at a distance of 3 mm from the base of the vial, containing 3.5 g double distilled water.

A typical relationship between the dielectric relaxation peak frequency and the temperature of ice is shown in ***Figure 11***. The fitting of polynomial functions to (1) the plot of log F_{PEAK} vs temperature and (2) the plot of temperature vs log F_{PEAK} (***Table 1)*** are used to generate a set of temperature coefficients which demonstrate the temperature dependence of F_{PEAK} parameter and a set of calibration coefficients which are expected to provide the basis for the prediction of the product temperature during primary drying.

Here, we introduce the parameter $T_{(F_{\mathrm{PEAK}})}$ to define those temperatures that predicted during the subsequent primary drying stage from the F_{PEAK} calibration that was recorded during the annealing stage.

Table 1 Temperature calibration parameters and temperature coefficients of the dielectric relaxation of ice within the TVIS vial

Order of fitting coefficient	2	1	0
Temperature calibration	−4.73E+00	−5.68E+01	−1.59E+02
Temperature coefficient	2.50E-04	5.07E-02	4.33E+00

Note: The temperature calibration parameters provide the means to predict temperature from log F_{PEAK} in the subsequent drying step; whereas the temperature coefficient defines the dependency of log F_{PEAK} on temperature.

Ice Formation (Nucleation and Growth)

Freeze-drying is a multi-stage process, which starts with the conversion of the majority of the liquid water to ice by super-cooling the solution below the solution melting point. The onset of ice nucleation, or rather the temperature at which the ice nucleates (T_n) is important to understanding how the ice structure develops, as it defines the size distribution of the interconnected pores and hence the porosity of the dry layer that is left behind once the ice has sublimed:

1. Slow freezing gives time for nucleation to occur at higher temperatures, by providing an extended period for ice nuclei to form around surfaces and foreign objects (particles in the solution). Nucleation at the higher temperatures then facilitates growth by maintaining water molecule mobility and hence diffusion to the ice front, and therefore the ice crystals which form are generally of a larger size which provides a more interconnected network of larger channels and therefore a lower dry layer resistance.
2. Fast freezing pushes the product to low temperature more rapidly and hence nucleation and then ice crystal growth tends to happen at lower temperatures which then reduces growth rates through a reduction in the rate of water molecule diffusion to the ice front, resulting in smaller ice crystals and a higher dry layer resistance.

It follows that the nucleation temperature is one of the critical process parameters in the design space (Arsiccio and Pisano 2018, 1586-1596). However, the stochastic nature of the process means that the nucleation onset temperature is difficult to control, unless additional technologies are deployed within the dryer such as the controlled nucleation technologies of pressure shock (Konstantinidis et al. 2011, 3453-3470) and ice fog (Rambhatla et al. 2004, 54-62). It is also important to note that in the sterile, particle free environment of a commercial scale freeze-dryer and with an aseptically filtered product one expects different nucleation behavior from the typical laboratory research tests within a less controlled environment.

It is a standard practice to measure the ice nucleation temperature with a product probe (i.e.

an RTD or thermocouple inserted in a test vial containing the product). However the probe itself alters the nucleation event by providing additional surfaces around which the nucleation event can occur while impacting the temperature in the vial as it provides an additional heat source. In effect the probe alters not only the process one is trying to measure (i.e. the nucleation onset temperature) but it will also impact the drying rate from that particular vial.

Photographic images of the nucleation event within a thermocouple vial and a TVIS vial are show in ***Figure 12***. In this particular example, it is clear that the ice is forming around the thermocouple whereas as in the TVIS vial the ice forms in the traditional manner of ice forming across the internal surface area of the vial.

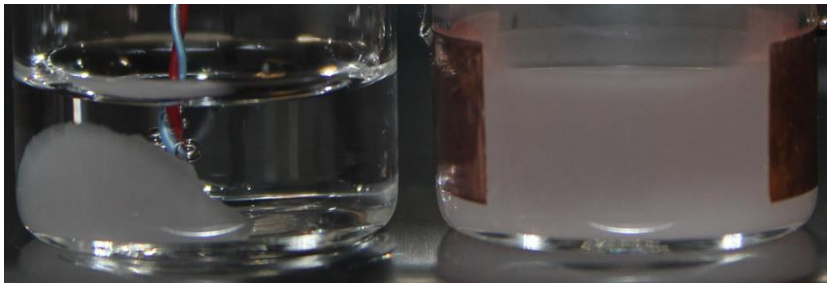

Figure 12 Ice forming occurring in a 10 mL type 1 glass tubing vial with thermocouple inside (Left) and the impedance measuring vial (Right) with an electrode pair (each 10 mm high and 19 mm wide, separated from the base by a 3 mm gap).

An example TVIS study of the ice nucleation and growth phase is shown in ***Figure 13***. Each graph focusses on a 2 hour time period during which the product temperature is reduced from ~0 °C to – 40 °C via a linear ramp of 0.5 °C min^{-1}. The 3D plots of real and imaginary capacitance vs frequency and time (***Figure 13a*** and ***13e***) capture the entire response surface and provide a first indication of what information might be extracted in terms of TVIS process parameters. These are the peak frequency (F_{PEAK}) and peak amplitude (C''_{PEAK}) from the imaginary capacitance spectra (***Figure 13a***) and the values for the real part capacitance at the limits of low and either side of the relaxation process. Here, we illustrate only the high frequency limit of the real part capacitance by selecting the time line for the 0.2 MHz frequency point (***Figure 13e***). We refer to this parameter as $C'(0.2\ \text{MHz})$, where the number in brackets signifies the experimental frequency chosen for analysis. These parameters are then plotted as a function of time during the freezing stage, in order

to establish which are sensitive to the onset of ice formation (nucleation) and which might be sensitive to the end of the ice solidification phase.

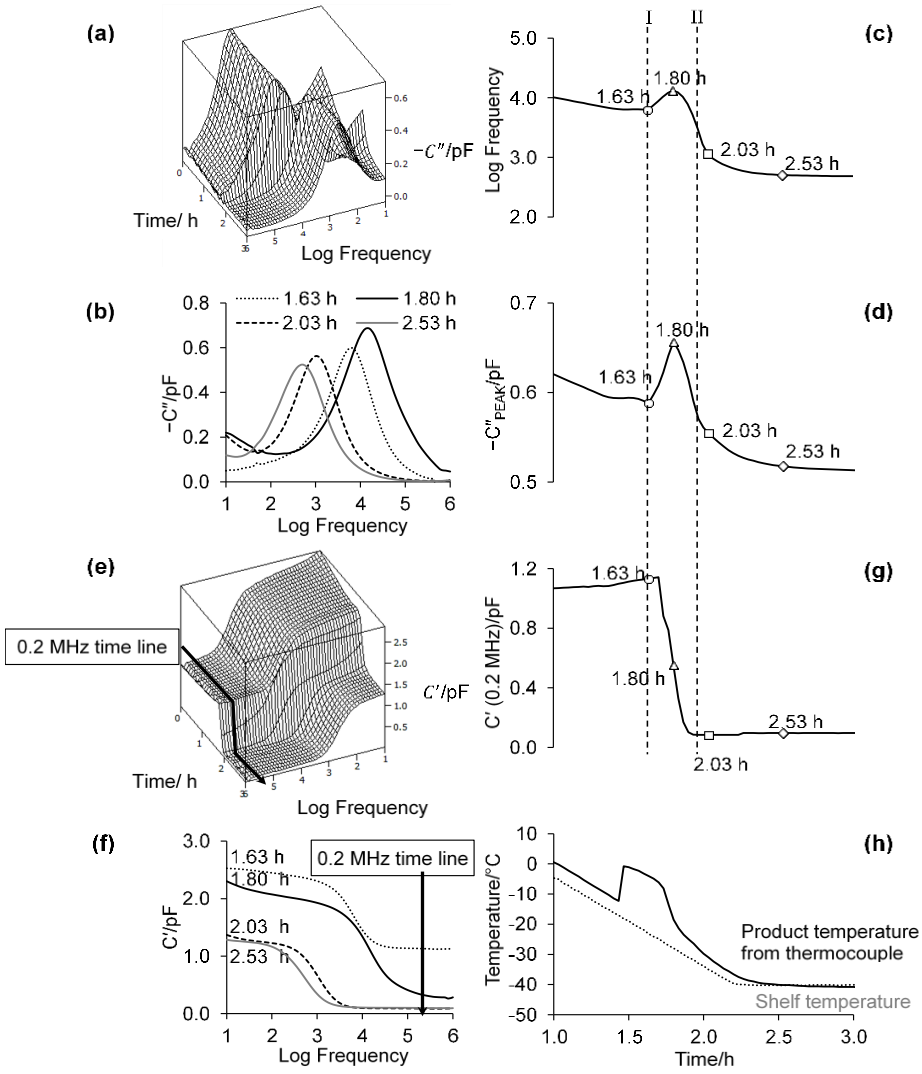

Figure 13 Freezing of two 10 mL type 1 glass-tubing vials placed adjacent to one another with each containing 3.5 g double distilled water. One has a pair of 10 x 19 mm electrodes attached to the outside wall of the vial at a height of 3 mm from the base. The other has a thermocouple immersed in the water. (a) and (e) are the response surfaces of the imaginary capacitance (dielectric loss) and real part capacitance (dielectric storage) as a function of frequency and time; (b) and (f) are the real and imaginary capacitance spectra at selected time points; (c) and (d) are the time profiles of the TVIS parameters F_{PEAK} and C''_{PEAK} ; (g) is the time profile of the TVIS parameter $C'(0.2\ \mathrm{MHz})$; (h) is the time profile of the thermocouple temperature. The ice nucleation event (at time point I) is reflected in the time profiles of both F_{PEAK} and C''_{PEAK} whereas the solidification end point (II) is reflected in the inflection in the real part capacitance measured at high frequency, $C'(0.2\ \mathrm{MHz})$.

From a close examination of Figure 13 it appears that the parameters of the TVIS response for water/ice that are most sensitive to the nucleation onset point are F_{PEAK} and C''_{PEAK}. At first glance, both appear to reflect the spike in temperature that is associated with the exothermic process of ice formation. However, the dielectric mechanisms responsible for these spikes are likely to be a complex function of the heterogeneous structures that co-exist during this phase transition as well, as the temperature dependencies of each structural domain. Some thoughts on these dielectric mechanisms are suggested here.

Given that ice forms from the bottom of the vial to the top of the vial then for at least part of the time period during which ice forms, there will be a residual liquid volume (albeit shrinking) on top of the ever increasing volume of the ice phase. The liquid that remains at any particular time can then provide in-part one of the mechanisms underpinning the spike in each parameter, through the positive temperature dependency of the relaxation frequency and capacitance increment of the Maxwell Wagner process associated with the liquid phase. However, that alone cannot be wholly responsible for the spikes in F_{PEAK} and C''_{PEAK} because the maximal increase in both F_{PEAK} and C''_{PEAK} exceeds the initial value at 0 °C and so there must be other more dominant mechanisms at play. One tentative suggestion is that the creation of intermediate ice structures prior to the completion of solidification across the liquid creates opportunities for further interfacial polarization effects within the bulk ice mass that collectively have higher dipole moments than the completely frozen ice mass.

For the case in which the TVIS vial nucleates before the thermocouple containing vial then the nucleation temperature in the TVIS vial can be 'read' simply from the average temperatures in the nearest neighbor vials. However, if the TVIS vial doesn't nucleate first then as soon as ice begins to nucleate in the nearest neighbor thermocouple vials, the resultant spike in temperature will inevitably preclude any further direct prediction of the temperature in the TVIS vial. In this case, the nucleation temperature in the TVIS vial may not be inferred directly from the thermocouple containing vials. However, by fitting a suitable curve to the plot of log F_{PEAK} against the average temperature from thermocouple vials ***(Figure 14)*** then it is possible to

extrapolate the curve to the nucleation point (i.e. when log F_{PEAK} starts to increase dramatically) in order to predict the nucleation temperature, T_n. In either case of the TVIS vial nucleating first or second, the fact that the TVIS vial doesn't contain an invasive thermocouple means that one can then consider the TVIS vial to be representative of vials placed at that location in the dryer in terms of the ice crystal structure that forms on freezing and the subsequent sublimation characteristics in the primary drying stage.

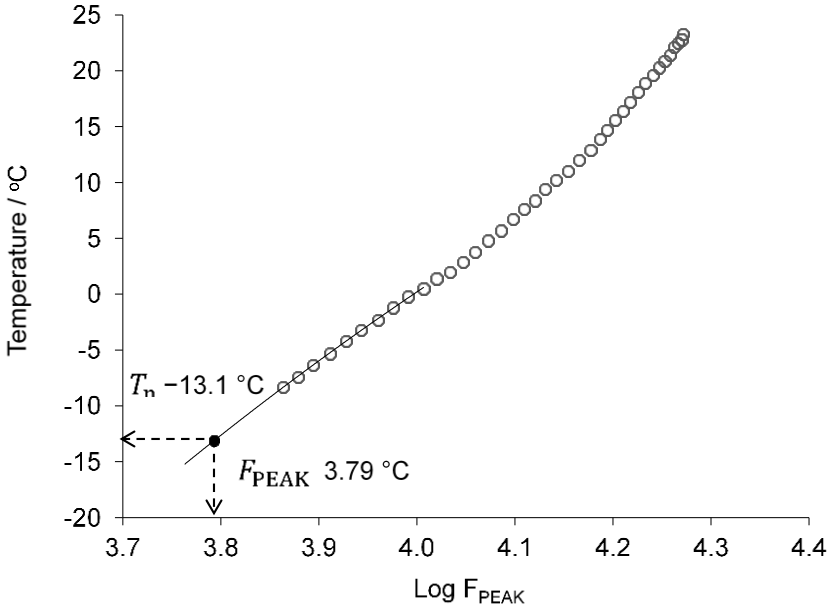

Figure 14 Prediction of ice nucleation temperature (T_n) by using a calibration plot between log F_{PEAK} and thermocouple temperature of ice within an adjacent vial.

Having described a non-invasive approach for the determination of the nucleation temperature we now describe an approach for the determination of the solidification end point; one that does not rely on any changes in the temperature of the contents of the vial. The reason why temperature is not ideal for the assessment of the solidification end point can be explained as follows: The freezing process, in many conventional cycles, comprises a slow ramp from a temperature above the freezing point to the solidification temperature. It is therefore likely that the solidification of ice is completed, in advance of the shelf temperature reaching its set value. Using a temperature sensor, such as a thermocouple, to predict the solidification end point is complicated by the fact that the temperature in the vial continues to change beyond the solidification end point, and so the end point is not so clear.

Here we exploit the fact that the high frequency real part capacitance of ice has a very low temperature coefficient (i.e. it does not change greatly with fluctuations in temperature). It follows that once all the ice has formed then the high frequency capacitance of the TVIS vial settles quickly to a value which remains almost constant, despite the fact that the temperature of the vial may continue to change as the system attempts to lose the excess latent heat that was generated on formation of the ice. This provides a more distinct end point for the completion of the solidification phase.

With the current instrument that was developed for TVIS measurements, and which has provided all the data for this chapter, there is some distortion to the high frequency end of the spectrum and so we have used the 200 kHz frequency point to determine the solidification end point. ***Figure 13e*** shows the response surface of the real part capacitance as functions of frequency and time. The solid black line highlights the time line for the 200 kHz frequency which is then shown in ***Figure 13g***. From Figure 13g one can easily recognize the solidification end point from the inflection where the steep descent in the real part capacitance transitions to an almost constant value (see vertical line II).

Conclusions

This chapter describes opportunities for using through vial impedance spectroscopy in the non-invasive measurement of the ice nucleation temperature and the end point of ice formation (complete solidification). The sensitivity of the TVIS dielectric loss peak to the formation of ice is due to the transition in the mechanism of relaxation from the Maxwell Wagner polarization of the glass wall (through the electrical resistance of the liquid water phase) to the dielectric relaxation of ice. During the crystallization of ice, it is inevitable that both the liquid and solid state will coexist during the period of time from the onset of ice formulation (nucleation) to the complete solidification of ice. Fortunately, the relaxation frequencies of both processes have positive temperature dependencies and so, regardless of how much of the water is in either of the liquid and solid states, one can expect the peak

frequency to be sensitive to the spike in temperature that originates from the release of latent heat, as the liquid transitions to the solid state (ice). This in effect underpins the use of the TVIS parameters in the determination of the nucleation onset time.

For the end point of ice formation we have proposed alternative approach to that based on the observation of a temperature spike, one, which instead uses temperature independent high frequency capacitance of ice.

In future publications we will extend this work to include the ice nucleation temperature and end points of the solidification of ice that forms from aqueous solutions. The issue to be addressed then, with using the dielectric loss peak for monitoring the ice formation process in conductive samples (such as a protein solution, a drug solution, or even a sugar solution with added salt) is that the peak frequency will be outside the frequency range of the instrument when the sample is in the initial liquid state. This is because the dielectric loss peak for the liquid state material is due to a Maxwell-Wagner (interfacial) polarization of the glass wall through the solution resistance and if the resistance of the solution is low then the loss peak frequency shifts to high frequency and the dielectric loss parameter then becomes less sensitive to any changes in the properties of the solution inside the vial. An alternative approach is therefore required.

Acknowledgments

The original TVIS system used to generate the spectra within this book chapter was developed by Evgeny Polygalov and Geoff Smith (from De Montfort University) in a collaboration with GEA Pharma Systems (Eastleigh, UK) and was part-funded by a UK government, Innovate UK Collaborative R&D project called LyoDEA (Project Reference: 10052

Bibliography

Arshad, Muhammad Sohail, Geoff Smith, Eugene Polygalov, and Irina Ermolina. 2014. "Through-Vial Impedance Spectroscopy of Critical Events during the Freezing Stage of the Lyophilization Cycle: The Example of the Impact of Sucrose on the Crystallization of Mannitol." *European Journal of Pharmaceutics and Biopharmaceutics* 87 (3): 598-605. doi:10.1016/j.ejpb.2014.05.005.

Arsiccio, A. and R. Pisano. 2018. "Application of the Quality by Design Approach to the Freezing Step of Freeze-Drying: Building the Design Space." *Journal of Pharmaceutical Sciences* 107 (6): 1586-1596.

Careri, G., M. Geraci, A. Giansanti, and J. A. Rupley. 1985. "Protonic Conductivity of Hydrated Lysozyme Powders at Megahertz Frequencies." *Proceedings of the National Academy of Sciences of the United States of America* 82 (16): 5342-5346.

Friess, W., M. Resch, and M. Wiggenhorn. 2010. *Monitoring Device for a Dryer* Google Patents.

Grassini, Sabrina, Marco Parvis, and Antonello A. Barresi. 2013. "Inert Thermocouple with Nanometric Thickness for Lyophilization Monitoring." *IEEE Transactions on Instrumentation and Measurement* 62 (5): 1276-1283.

Horn, Jacqueline and Wolfgang Friess. 2018. "Detection of Collapse and Crystallization of Saccharide, Protein and Mannitol Formulations by Optical Fibers in Lyophilization." *Frontiers in Chemistry* 6.

Kasper, Julia Christina, Michael Wiggenhorn, Manfred Resch, and Wolfgang Friess. 2013. "Implementation and Evaluation of an Optical Fiber System as Novel Process Monitoring Tool during Lyophilization." *European Journal of Pharmaceutics and Biopharmaceutics* 83 (3): 449-459.

Konstantinidis, Alex K., Wei Kuu, Lori Otten, Steven L. Nail, and Robert R. Sever. 2011. *Controlled Nucleation in Freeze-drying: Effects on Pore Size in the Dried Product Layer, Mass Transfer Resistance, and Primary Drying Rate*. Vol. 100. doi:https://doi.org/10.1002/jps.22561.

Nail, Steven, Serguei Tchessalov, Evgenyi Shalaev, Arnab Ganguly, Ernesto Renzi, Frank Dimarco, Lindsay Wegiel, Steven Ferris, William Kessler, and Michael Pikal. 2017. "Recommended Best Practices for Process Monitoring Instrumentation in Pharmaceutical Freeze drying—2017." *AAPS PharmSciTech* 18 (7): 2379-2393.

Parvis, Marco, Sabrina Grassini, and Antonello Barresi. 2012. "Sputtered Thermocouple for Lyophilization Monitoring."Instrumentation and Measurement Technology Conference (I2MTC), 2012 IEEE International.

Parvis, Marco, Sabrina Grassini, Daniele Fulginiti, Roberto Pisano, and Antonello A. Barresi. 2014. "Sputtered Thermocouple Array for Vial Temperature Mapping."Instrumentation and Measurement Technology Conference (I2MTC) Proceedings, 2014 IEEE International

Popov, Ivan, Ivan Lunev, Airat Khamzin, Anna Greenbaum, Yuri Gusev, and Yuri Feldman. 2017. "The Low-Temperature Dynamic Crossover in the Dielectric Relaxation of Ice I H." *Physical Chemistry Chemical Physics* 19 (42): 28610-28620.

Popov, Ivan, Alexander Puzenko, Airat Khamzin, and Yuri Feldman. 2015. "The Dynamic Crossover in Dielectric Relaxation Behavior of Ice I H." *Physical Chemistry Chemical Physics* 17 (2): 1489-1497.

Rambhatla, Shailaja, Roee Ramot, Chandan Bhugra, and Michael J. Pikal. 2004. "Heat and Mass Transfer Scale-Up Issues during Freeze Drying: II. Control and Characterization of the Degree of Supercooling." *AAPS PharmSciTech* 5 (4): 54-62.

Roy, M. L. and M. J. Pikal. 1989. "Process Control in Freeze Drying: Determination of the End Point of Sublimation Drying by an Electronic Moisture Sensor." *Journal of Parenteral Science and Technology : A Publication of the Parenteral Drug Association* 43 (2): 60-66.

Schneid, S. and H. Gieseler. 2008. "Evaluation of a New Wireless Temperature Remote Interrogation System (TEMPRIS) to Measure Product Temperature during Freeze Drying." *AAPS PharmSciTech* 9 (3): 729-739.

Smith, G. and E. Polygalov. "Chapter 11. through Vial Impedance Spectroscopy (TVIS): A Novel Approach to Process Understanding for Freeze-Drying Cycle Development." In *Lyophilization of Pharmacueuticals, Vaccines and Medical Diagnostics,* edited by Kevin Ward and P. Matejtschuk. New York: Springer.

Smith, Geoff, Muhammad Sohail Arshad, Eugene Polygalov, and Irina Ermolina. 2014. "Through-vial Impedance Spectroscopy of the Mechanisms of Annealing in the Freeze-drying of Maltodextrin: The Impact of Annealing Hold Time and Temperature on the Primary Drying Rate." *Journal of Pharmaceutical Sciences* 103 (6): 1799-1810.

Smith, Geoff, Muhammad Sohail Arshad, Eugene Polygalov, Irina Ermolina, Timothy R. McCoy, and Paul Matejtschuk. 2017. "Process Understanding in Freeze-Drying Cycle Development: Applications for through-Vial Impedance Spectroscopy (Tvis) in Mini-Pilot Studies." *Journal of Pharmaceutical Innovation* 12 (1): 26-40.

Smith, Geoff, Muhammad Sohail Arshad, Eugene Polygalov, and Irina Ermolina. 2013. "An Application for Impedance Spectroscopy in the Characterisation of the Glass Transition during the Lyophilization Cycle: The Example of a 10% W/V Maltodextrin Solution." *European Journal of Pharmaceutics and Biopharmaceutics* 85 (3, Part B): 1130-1140.

Smith, Geoff, Yowwares Jeeraruangrattana, and Irina Ermolina. 2018. *The Application of Dual-Electrode through Vial Impedance Spectroscopy for the Determination of Ice Interface Temperatures, Primary Drying Rate and Vial Heat Transfer Coefficient in Lyophilization Process Development*. Vol. 130. doi:https://doi.org/10.1016/j.ejpb.2018.05.019.

Suherman, Phe Man. 2001. "A Novel Dielectric Technique for Monitoring the Lyophilisation of Globular Proteins." Doctoral, De Montfort University.

Suherman, Phe Man, Peter M. Taylor, and Geoff Smith. 2002. "Development of a Remote Electrode System for Monitoring the Water Content of Materials Inside a Glass Vial." *Pharmaceutical Research* 19 (3): 337-344. doi:10.1023/A:1014455304527.